Thin Solid Films 527 (2013) 164–169

Contents lists available at SciVerse ScienceDirect

Thin Solid Films

journal homepage: www.elsevier.com/locate/tsf

Effect of thickness on optical properties of thermally evaporated SnS films

M.S. Selim [a], M.E. Gouda [b,*], M.G. El-Shaarawy [b], A.M. Salem [a,c], W.A. Abd El-Ghany [a]

[a] Electron Microscope and Thin Films Dept., Physics Division, National Research Center, Cairo, Egypt
[b] Physics Dept., Faculty of Science, Benha University, Banha, Egypt
[c] Physics Department — University College — Alqunfoza — Umm Al-Qura University — Saudi Arabia

ARTICLE INFO

Article history:
Received 31 December 2011
Received in revised form 13 October 2012
Accepted 16 October 2012
Available online 23 October 2012

Keywords:
Optical properties
Thin films
Selenium sulfide
Evaporation

ABSTRACT

The effect of film thickness on the structure and optical properties of thermally evaporated SnS film has been studied. SnS films with different thicknesses in the range 152–585 nm were deposited onto clean glass substrates at room temperature. X-ray diffraction study revealed that SnS films of thickness ≥283 nm are crystalline, whereas films of lower thickness exhibit poor crystalline with more amorphous background. The crystalline nature of the lower film thickness has been confirmed using transmission electron microscope and the corresponding electron diffraction pattern. The thicker film samples showed nearly stoichiometric chemical composition; however, thinner samples are deficient in S and rich in Sn. The optical property of the deposited films has been investigated in the wavelength range 350–2500 nm. The refractive index increases notably with increasing film thickness. The refractive index for the investigated film thicknesses are adequately described by the effective-single-oscillator model. The static refractive index and the static dielectric constant have been calculated. Analysis of the optical absorption coefficient revealed the presence of direct optical transition and the corresponding band gap values were found to decrease as the film thickness increases.

1. Introduction

Recent investigations on photovoltaic materials have shown considerable interest in SnS thin films [1–3] and other optoelectronic devices like holographic recording system [4], solar control device [5] and near-infrared detector [6].

SnS belongs to the IV–VI compounds whose constituent elements are abundant in nature. It crystallizes in an orthorhombic structure as a deformed sodium chloride structure and is a layered material that presents interesting semiconducting properties [7]. It has different optical band gap values ranging from 1 to 2.33 eV depending on the resulting structure obtained by different techniques and the occurring type of electron transitions [8–10].

For photovoltaic applications *p*-type SnS being the absorber material requires an *n*-type wide band gap transparent semiconductor as the heterojunction partner [3]. Essentially among all known transparent semiconductor, non-stoichiometric or doped oxides and sulfides such as SnO_2, ZnO, CdS and ZnS, the p-type SnS may be the best choice for *n*-type material as a heterojunction partner. The performance of such heterojunction partners is strongly limited by the thickness and various characteristic properties of deposited SnS films. The change of material properties particularly with film thickness could be due to the variation of the crystal size. The influence of the crystal size on the physical properties has aroused much interest in semiconductor devices. The structure of the deposited films changes with the change of the film thickness, which will in turn affect the optical transmittance and the electronic properties of the deposited films [11–13]. A study of properties in relation to the film thickness has great importance in order to obtain films that are capable to assure stable and efficient device performance.

In the present work, we study the effect of film thickness on the structure and optical properties of thermally evaporated SnS films deposited onto glass substrates.

2. Experimental technique

SnS thin films of different thicknesses were deposited from the pre-synthesized ingot material via thermal evaporation technique onto clean glass substrates at room temperature. The deposition process was carried out using a high vacuum coating unit (Type Edwards, E306A) in a vacuum pressure of ~2×10^{-4} Pa. The deposition rate (3–7 nm·s^{-1}) and the thickness of the deposited films were controlled during deposition process by means of quartz crystal thickness monitor (Type Edwards, FTM4).

The structural characteristics of the deposited films were examined using an X-ray diffraction (XRD-Philips X'pert) operating at 40 kV and 30 mA, with CuKα radiation of wavelength λ = 0.15406 nm. The measurements were conducted at 2θ diffraction angles from 10° to 80°, with a step size of 0.04°. The microstructure and chemical composition of thinner film sample was investigated using transmission electron microscope (TEM) (Type JEOL JEM-1230) operating at 120 kV, interfaced with energy dispersive X-ray spectrometry unit. For this task, thin film

* Corresponding author.
E-mail address: mostafagouda88@yahoo.com (M.E. Gouda).

0040-6090/$ – see front matter
http://dx.doi.org/10.1016/j.tsf.2012.10.019

of thickness ~100 nm (suitable for TEM investigation) was deposited onto clean glass substrate. The film was stripped from the glass substrate by immersing the substrate covered with film gently on the surface of double distilled water in a glass dish. The film was then floated onto the water surface and fished onto a microscopic copper grid. On the other hand, the chemical composition for thicker film sample was examined using energy dispersive X-ray spectrometry unit (Type INCA x-sight Oxford England) interfaced with a scanning electron microscope (Type JOEL JEM-850) operating with an accelerating voltage of 30 kV, with an estimated average precision of 3% in atomic fraction in each element.

A double beam spectrophotometer, with automatic computer data acquisition (Type Jasco, V-570, Rerll-00, UV–VIS–NIR) was used at normal light incidence to record the optical transmission and reflection spectra of the deposited films over the wavelength range 350–2500 nm. The measurements were made at room temperature on various parts of the deposited films, scanning the entire sample, and a very good reproducibility of the spectra was generally achieved.

3. Results and discussions

3.1. Structural characterization of the deposited films

3.1.1. X-ray diffraction analysis

The XRD patterns of as-deposited SnS films (of different film thicknesses) deposited onto glass substrates at room temperature are shown in Fig. 1. The XRD pattern revealed that the as-deposited SnS films of thicknesses 283 and 470 nm show a prominent peak at $2\theta = 31.66°$ corresponding to the (111) plane that matched well with the orthorhombic structure as compared to the JCPDS card no. 39–0354. With an increase of thickness to 585 nm, the film showed another reflection peak observed at $2\theta = 30.62°$ corresponding to (101) plane. The intensity of the (111) diffraction peak becomes more intense and sharp with the increase of the film thickness, which indicates an improvement in the crystallinity of the deposited films. In general, an increase of film thickness increases the probability of crystallization [14]. On the other hand, as-deposited SnS films of thickness 152 and 225 nm did not indicate clearly whether the films are amorphous or crystalline due to the absence of any observable peaks in such patterns. Further analysis was performed using the transmission electron microscope and electron diffraction to identify clearly whether SnS films of thinner thicknesses are amorphous or crystalline.

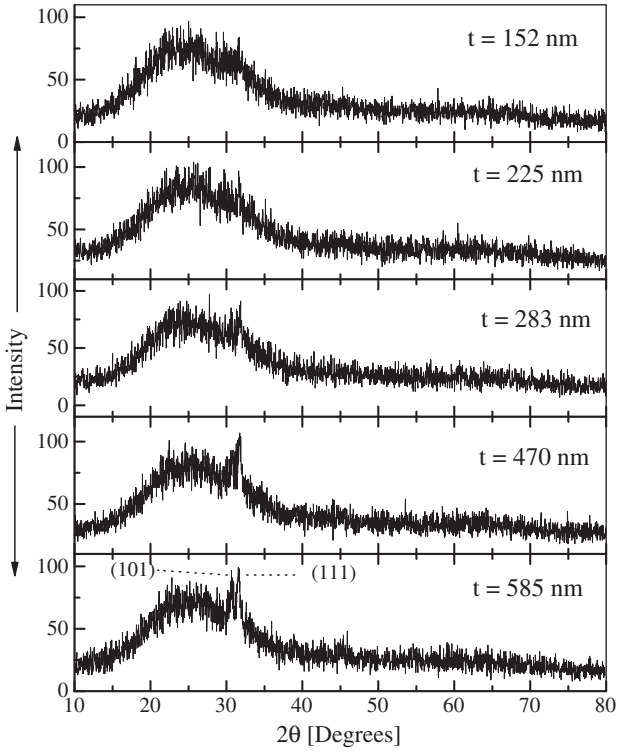

Fig. 1. X-ray diffraction patterns of as-deposited SnS films of different thicknesses.

Fig. 2 shows the TEM micrograph and the corresponding electron diffraction pattern of as-deposited SnS film of thickness 100 nm. The transmission electron micrograph revealed that the as-deposited SnS films showed needle-like crystallites which are tightly bonded together forming a continuous dense network. The corresponding electron diffraction pattern showed continues faint rings confirming the crystalline nature of the as-deposited SnS films. Therefore, the absence of any observable peaks in the XED patterns for SnS films of thickness lower than 283 nm was attributed to crystal size effect.

3.1.2. Chemical analysis of the deposited SnS films

Fig. 3 shows the energy dispersive X-ray spectrum of representative SnS film corresponding to lower (100 nm) film thickness. The spectrum showed peaks corresponding to the elements Sn and S, beside other peaks observed at 0.93, 1.1, 8.05, and 8.98 eV coming from the copper grid. However, the spectrum for the sample of thickness 585 nm deposited onto glass substrate (not given here) showed only sharp peaks related to Sn and S in addition to Si peak observed at 1.74 eV coming from the glass substrate. The variation of Sn to S atomic ratio of SnS films with respect to lower and higher film thickness are listed in Table 1. It is clearly seen from the data reported in Table 1, that the compositional ratio of the as-deposited SnS film of thickness 585 nm was nearly stoichiometric. However, SnS film of lower film thickness (100 nm) was found poor in S and rich in Sn, which indicates non-stoichiometric composition. This finding could be attributed to the long Sn–S bond in the crystal structure, which is responsible for the release of sulfur in the case of as-deposited thinner SnS films [1].

3.2. Optical properties of SnS films

Fig. 4 shows the transmittance and reflectance spectra obtained for SnS with different film thicknesses. It is seen that the transmittance spectra for SnS films of thickness 470 and 585 nm exhibited sharp fall (sharp absorption edge) around 580 nm, indicating a good homogeneity in the grain shape and size, and low defect concentration in the films. However, the transmission spectra for the samples of thickness $t = 152$, 250 and even for 255 nm showed strange shape with no sharp band edge i.e. exhibit a cut off on the T spectrum at short wavelengths. This behavior was attributed to the poor crystallinity and/or optical homogeneity of these films. The strange shape of the optical transmission spectra at shorter wavelength side has been also observed for thermally evaporated SnS films [15,16]. The growth of thin films by thermal evaporation process goes mainly through the composition of islands, network and continuous stages where, the crystallite sizes of the deposited films increase with increasing film thickness. Therefore, the increase of the film thickness in the present work enhances the film crystallization, and hence the optical homogeneity. It was also observed that in the near-infrared spectral region when the transmission increases the reflection decreases, indicating that some light attenuation occurs due to scattering process.

The optical properties of the deposited SnS films may be represented by the refractive index, n, and extinction coefficient, k, which are the real and imaginary parts of the complex refractive index $N = n\text{-}ik$, respectively. In the case of normal light incident the values of n and k were computed using a film thickness, t, and both recorded values of

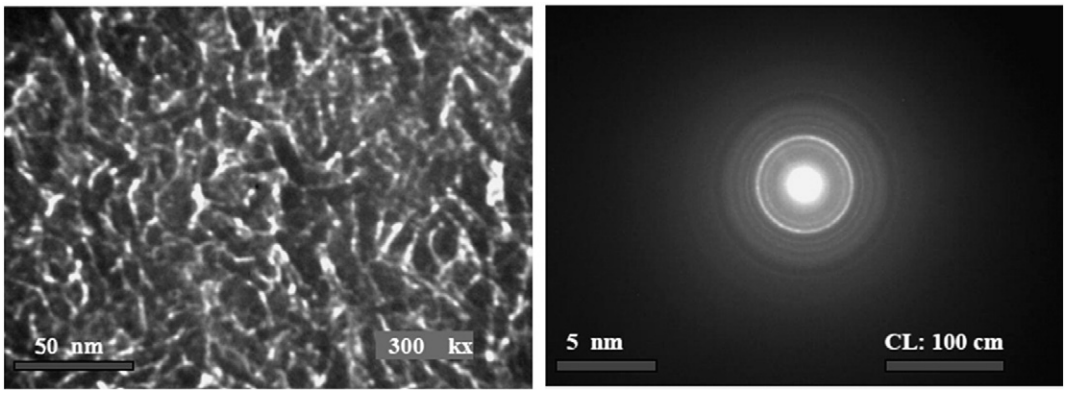

Fig. 2. TEM and the corresponding electron diffraction patterns of as-deposited SnS film of thickness 100 nm.

transmission and reflection spectra in the investigated wavelength optical range according to the Murmann's exact equations [17,18]:

$$R = \frac{Ae^{\beta} + B^{-\beta} + 2C\cos\alpha + 4D\sin\alpha}{Ee^{\beta} + Fe^{-\beta} + 2G\cos\alpha + 4H\sin\alpha} \quad (1)$$

$$T = \frac{16n_o n_s\left(n^2 + k^2\right)}{Ee^{-\beta} + Fe^{-\beta} + 2G\cos\delta + 4H\sin\alpha} \quad (2)$$

where

$$A = \left[(n-n_s)^2 + k^2\right]\left[(n+n_s)^2 + k^2\right]$$

$$B = \left[(n-n_s)^2 + k^2\right]\left[(n+n_o)^2 + k^2\right]$$

$$C = \left(n^2 + k^2\right)\left(n_o^2 + n_s^2\right) - \left(n^2 + k^2\right)^2 - n_o^2 n_s^2 - 4n_o n_s k^2$$

$$D = k(n_s - n_o)\left(n^2 + k^2 + n_o n_s\right)$$

$$E = \left[(n+n_o)^2 + k^2\right]\left[(n+n_s)^2 + k^2\right]$$

$$F = \left[(n-n_o)^2 + k^2\right]\left[(n-n_s)^2 + k^2\right]$$

$$G = \left(n^2 + k^2\right)\left(n_o^2 + n_s^2\right) - \left(n^2 + k^2\right)^2 - n_o^2 n_s^2 + 4n_o n_s k^2$$

$$H = k(n_s + n_o)\left(n^2 + k^2 - n_o n_s\right); \propto = 4\pi nt/\lambda \text{ and } \beta = 4\pi kt/\lambda$$

where $n_o = 1$ is the refractive index of air, n_s is the refractive index of the substrate, t is the film thickness, and λ is the wavelength of the incident beam. Murmann's exact equations require initial guessed value of the film refractive index, n_i and extinction coefficient, k_i. The guessed value of n_i was calculated from the experimental value of R at longer wavelength (2500 nm) using the relation; $n_i = (1+\sqrt{R}) \,/\, (1\text{-}\sqrt{R})$ and the guessed value of k_i is estimated using the equation; $exp((4\pi k_i t)/\lambda) = (1\text{-}R)/T$. Initial values of n_i and k_i (especially n_i) must be properly chosen for a physically meaningful solution to be obtained.

Therefore, using the experimental values of the transmission T_{exp} and reflectance R_{exp}, one can solve Murmann's exact equations, namely $f_r(n, k) = R(n, k) - R_{exp} = 0$ and $f_t = T(n, k) - T_{exp} = 0$, simultaneously to obtain accurate values of the film refractive index, n and extinction coefficient, k using a special iterative computer program [19].

Fig. 5 shows the spectral variation of the refractive index as a function of wavelength for SnS films for different thicknesses. The figure depicts that the refractive index n attains a peak in the absorption region (below 950 nm), which shifts towards higher wavelengths as the film thickness increases. Beyond the observed peaks the refractive index for different film thicknesses decreases with increasing wavelength and becomes fairly flat above 1500 nm, showing normal dispersion behavior. In addition, the magnitude of refractive index increases notably with increasing the film thickness. The lower value of refractive index for thinner films might be due to the poor packing density of the deposited layers [20,21].

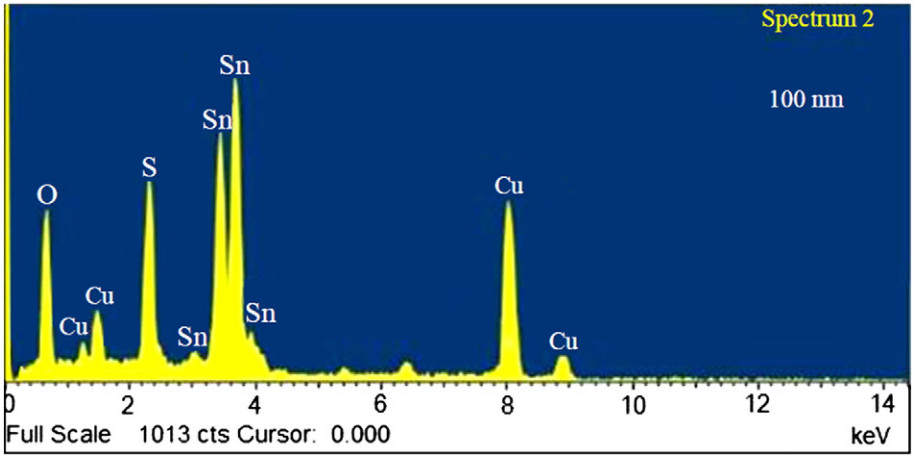

Fig. 3. Energy dispersive X-ray spectrum of film thickness 100 nm.

Table 1
Chemical composition (at %) results and Sn/S ratios of SnS films of two representative film thicknesses, with a precision of 3% in atomic fraction in each element.

Element	Film thickness	
	t = 585 nm	t = 100 nm
Sn	51	58
S	49	42
Sn/S	1.04	1.38

The data of the dispersion refractive index, n (λ), may be analyzed using the single-effective-oscillator Wemple and DiDomenico model [22]. The model suggests that the data could be described by:

$$n^2(\nu) = 1 + \frac{E_o E_d}{E_o^2 - (h\nu)^2} \quad 3$$

where $\hbar = h/2\pi$ (h is Planck's constant), ($\hbar\,\omega$) is the photon energy, E_o is the oscillator energy and E_d is the dispersion energy or the oscillator strength.

The oscillator energy, E_o is an "average" energy gap and can be related to the optical band gap E_g in close approximation by $E_o \approx 2\,E_g$ [23]. On the other hand, the dispersion energy, E_d, is a measure of the strength of interband optical transitions and can be considered as a parameter having very close relation with the charge distribution within the unit cell and therefore with the chemical bonding. This parameter follows a simple empirical relationship of the form [22]:

$$E_d = \beta N_c N_e Z_a \quad 4$$

where β is a constant whose value depends on the chemical bonding character of a material, N_c is the coordination number of the cation nearest-neighbor to the anion, Z_a is the formal chemical valency of the anion, and N_e is the total number of valence electrons per anion.

Therefore, plotting $(n^2-1)^{-1}$ against photon energy, $(h\nu)^2$ and fitting a linear function to smaller energy data as shown in Fig. 6 allows the determination of the oscillator parameters, E_o, and E_d. The calculated values of E_o, and E_d, static refractive index, $n_s(0) = (1 + E_d/E_o)^{1/2}$ as well as the static dielectric constant, $\varepsilon_s = n_s^2(0)$ for different SnS film thickness are listed in Table 2. It is clearly seen from the data reported in Table 2 that, the oscillator energy E_o varies in a reverse manner to the calculated values of E_d and $n_s(0)$. The observed decrease in the values E_o with increasing SnS film thickness can be attributed to the observed red shift of the optical transmission spectra in the short wavelengths spectral region (see Fig. 4). The calculated values of the oscillation parameter E_o are in a agreement with the corresponding values reported in Ref. [24]. On the other hand, the observed increase in the values of E_d with increasing film thickness can be attributed to the variation of the coordination number of the cation nearest-neighbor to the anion which mainly depends on the chemical composition of the deposited films and/or to the increased crystalline nature of the thicker film samples. It is worth mentioning here that the E_o value gives quantitative information on the overall band structure of the material. This is in fact quite different from the information coming from the value of the optical gap, E_g calculated from the fundamental absorption edge (as will be mentioned below).

The low wavelength absorption data for the as-deposited SnS films are related to the fundamental absorption which refers to the band-to-band transition, i.e. to the excitation of an electron from the valence band to the conduction band. The absorption coefficient, α calculated using the above mentioned relations for different film thicknesses are shown in Fig. 7. It is seen that the absorption coefficient of the investigated film thickness range varies between $3\times10^3 - 4\times10^4 \mathrm{cm}^{-1}$.

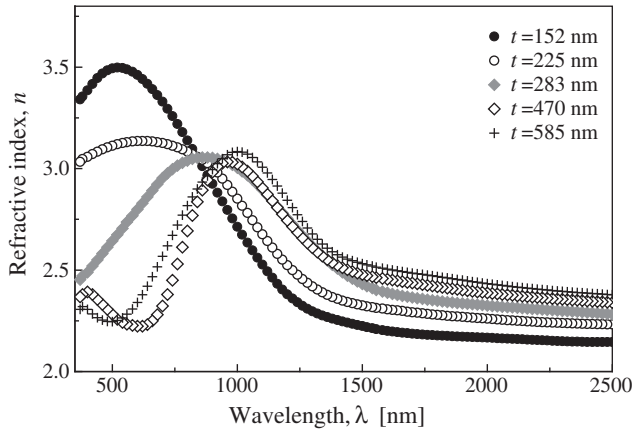

Fig. 5. Spectral variation of the refractive index vs. wavelength for SnS films with different thicknesses.

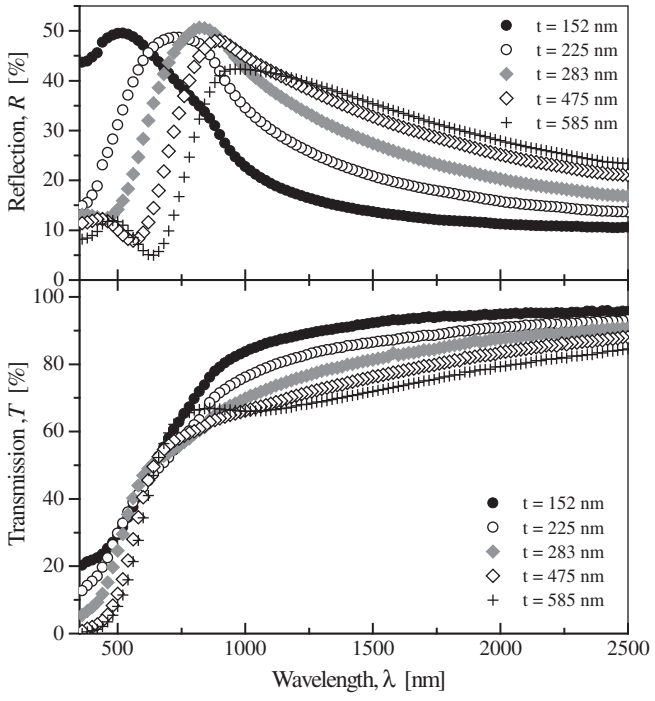

Fig. 4. Transmission and reflection spectra of as-deposited SnS films of different thicknesses.

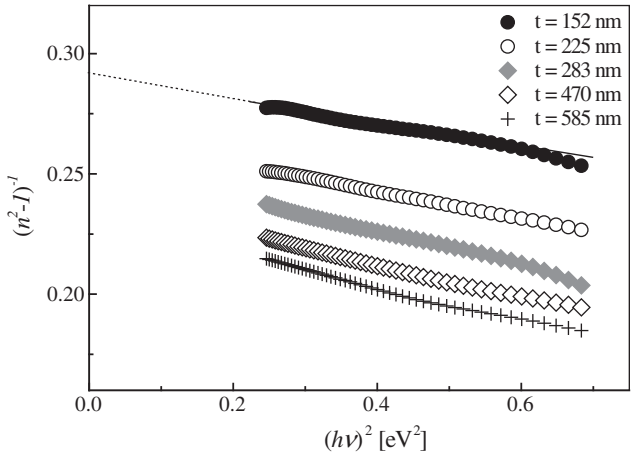

Fig. 6. Plots of $(n^2\text{-}1)^{-1}$ vs. photon energy squared.

Table 2
Optical parameters of SnS films of different thicknesses.

Film thicknesses [nm]	E_d (±0.5 eV)	E_o (±0.3 eV)	$n_s(0)$	ε_s	$E_g^{W.D}$ [eV]	$E_g^{dir.}$ (±0.05 eV)
155	15.48	4.17	2.172	4.726	2.08	1.68
225	15.71	3.86	2.252	5.072	1.93	1.62
283	16.44	3.59	2.359	5.566	1.79	1.62
470	16.53	3.34	2.438	5.946	1.67	1.43
585	17.98	3.25	2.555	6.529	1.63	1.36

The optical band gaps, E_g, values are calculated by assuming a direct transition between the edges of the valence and the conduction bands, for which the variation of the absorption coefficient, α, with photon energy is given by [24,25]:

$$(\alpha h\nu) = A\left(h\nu - E_g^{opt.}\right)^{1/2}. \quad 5$$

By plotting $(\alpha h\nu)^2$ versus $(h\nu)$ and extrapolating the linear region of the resulting curve as shown in Fig. 8 a, b, E_g can be obtained. It is seen that the optical band gap of SnS films decreased from 1.68 to 1.36 eV with increase of the film thickness from 152 to 585 nm. The decrease in optical band gap energy with the increase of the film thickness can be likely attributed to an improvement in the crystallinity of the deposited films as indicated from the XRD analysis. The estimated band gap value for different film thicknesses is also listed in Table 2.

4. Conclusions

SnS films with different thicknesses have been prepared onto clean glass substrates by thermal evaporation technique. The X-ray study revealed that SnS films of thickness ≥283 nm are crystalline, whereas films of lower thickness exhibit poor crystalline with more amorphous background. The crystalline nature of the lower film thickness has been confirmed using transmission electron microscope and the corresponding electron diffraction pattern. The chemical composition of thicker films samples showed nearly stoichiometric pattern, however, thinner samples are deficient in S and rich in Sn. The refractive index increases notably with increasing film thickness. Analysis of the refractive index dispersion on the basis of the Wemple and DiDomenico model showed that a reduction in the values of the oscillator energy E_o has been observed as the film thickness increases in a reverse manner to the values of E_d and also with the static refractive index n_s (0). Analysis of the optical absorption coefficient revealed the presence of direct optical transition. The calculated optical band gap values of the deposited SnS films have decreased from 1.68 to 1.36 eV with increasing the film thickness from 152 to 585 nm.

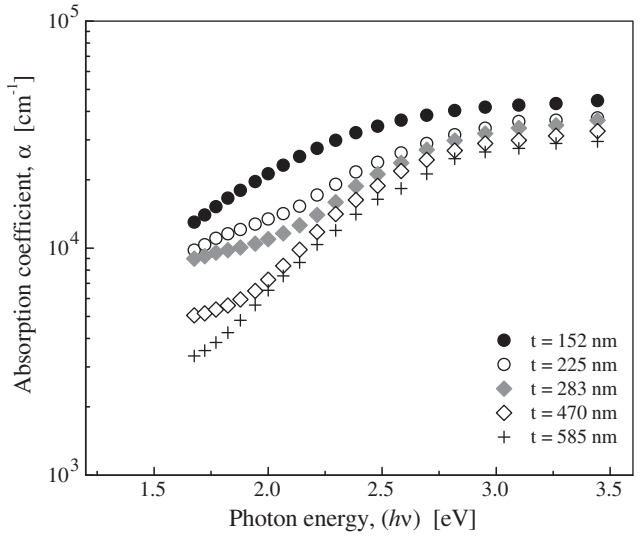

Fig. 7. Spectral variation of the absorption coefficients vs. photon energy for SnS films of different thicknesses.

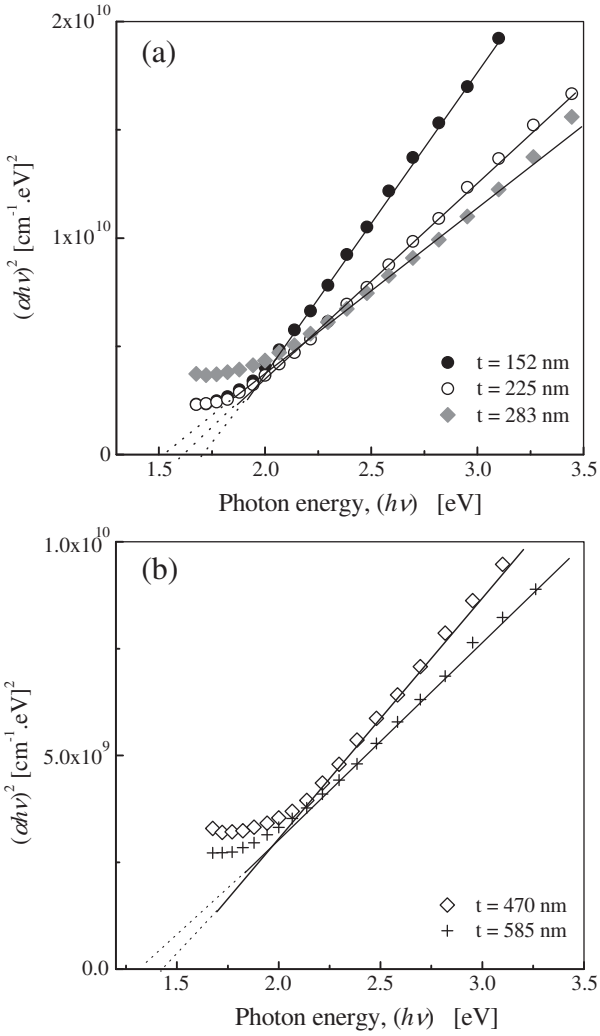

Fig. 8. a and b show the plots of $(\alpha h\nu)^2$vs. $(h\nu)$ for SnS films of different thicknesses.

Acknowledgments

The author's present their sincere gratitude to Prof. Dr. G. B. Sakr, Prof. of solid state and thin films physics, Faculty of Education, Ain Shams University, Cairo, Egypt for calculating the optical constant of the deposited films using his private computer program. Also, we would like to thank Prof. Dr. A. A. Fakhry for reviewing the manuscript.

References

[1] G. Biswajit, R. Bhattacharjee, P. Banerjee, S. Das, Appl. Surf. Sci. 257 (2011) 3670.
[2] M. Ristov, G. Sinadinovski, M. Mitreski, M. Ristova, Sol. Energy Mater. Sol. Cells 69 (2001) 17.
[3] B. Ghosh, M. Das, P. Banerjee, S. Das, Sol. Energy Mater. Sol. Cells 92 (2008) 1099.
[4] M. Radot, Rev. Phys. Appl. 18 (1977) 345.
[5] P.K. Nair, M.T.S. Nair, J. Phys. D Appl. Phys. 24 (1991) 83.
[6] P.M. Nikolic, D.M. Todorovic, J. Phys. C Solid State Phys. 20 (1987) 39.
[7] Li Qing, Yi Ding, Hao Wu, Xianming Liu, Yitai Qian, Mater. Res. Bull. 37 (2002) 925.
[8] M.M. El-Nahass, H.M. Zeyada, M.S. Aziz, N.A. El-Ghamaz, Opt. Mater. 20 (2002) 159.

[9] N. Koteswara Reddy, K.T. Ramakrishna Reddy, Thin Solid Films 325 (1998) 4.
[10] A. Ghazali, Z. Zainal, M.Z. Hussein, A. Kasseim, Sol. Energy Mater. Sol. Cells 55 (1998) 237.
[11] F. Lai, H. Li, H. Wang, Li Paggel, T.C. Chiange, Phys. Rev. Lett. 88 (2002) 256802.
[12] R. Bruggeman, P. Reinig, M. Holling, Thin Solid Films 427 (2003) 358.
[13] Z. Qiao, R. Latz, D. Msrgel, Thin Solid Films 466 (2004) 250.
[14] V.I. Trofimov, I.V. Trofimov, J. Kim, Thin Solid Films 495 (2006) 398.
[15] M. Devika, N. Koteeswara Reddy, D. Sreekantha Reddy, Q. Ahsanulhaq, K. Ramesh, E.S.R. Gopal, K.R. Gunasekhar, Y.B. Hahn, J. Electrochem. Soc. 155 (2008) H130.
[16] P.A. Nwofe, K.T. Ramakrishna Reddy, J.K. Tan, I. Forbes, R.W. Miles, Phys. Procedia 25 (2012) 150.
[17] O.S. Heavens, Optical Properties of Thin Solid Films, Dover, New York, 1965.
[18] O.S. Heavens, in: G. Hass, R. Thus (Eds.), Physics of Thin Films, Academic Press, New York, 1964.
[19] S.S. Fouad, G.B. Sakr, I.S. Yahia, D.M. Abdel Basset, Mater. Res. Bull. 46 (2011) 2141.
[20] V. Gupta, A. Mansingh, J. Appl. Phys. 80 (1996) 1063.
[21] N. Revathi, P. Prathap, K.T. Ramakrishna Reddy, . a Solid State Sci. 11 (2009) 1288 (b).
[22] S.H. Wemple, M. Didomenico, Phys. Rev. B 3 (1971) 1338.
[23] K. Tanaka, Thin Solid Films 66 (1980) 271.
[24] A.E. Abdelrahman, W.M.M. Yunus, A.K. Arof, J. Non-Cryst. Solids 358 (2012) 1447.
[25] J.I. Pankove, Optical Processes in Semiconductors, Dover, New York, 1975.